HIGH RESOLUTION TREE-RING BASED SPATIAL RECONSTRUCTIONS OF SNOW AVALANCHE ACTIVITY IN GLACIER NATIONAL PARK, MONTANA, USA

Gregory T. Pederson[(1,2)]*, Blase A. Reardon[(1)], Christian J. Caruso[(1,2)], and Daniel B. Fagre[(1)]

[(1)]U.S. Geological Survey – Northern Rocky Mountain Science Center, West Glacier, MT
[(2)]Big Sky Institute – Montana State University, Bozeman, MT

ABSTRACT: Effective design of avalanche hazard mitigation measures requires long-term records of natural avalanche frequency and extent. Such records are also vital for determining whether natural avalanche frequency and extent vary over time due to climatic or biophysical changes. Where historic records are lacking, an accepted substitute is a chronology developed from tree-ring responses to avalanche-induced damage. This study evaluates a method for using tree-ring chronologies to provide spatially explicit differentiations of avalanche frequency and temporally explicit records of avalanche extent that are often lacking. The study area - part of John F. Stevens Canyon on the southern border of Glacier National Park – is within a heavily used railroad and highway corridor with two dozen active avalanche paths. Using a spatially geo-referenced network of avalanche-damaged trees (n=109) from a single path, we reconstructed a 96-year tree-ring based chronology of avalanche extent and frequency. Comparison of the chronology with historic records revealed that trees recorded all known events as well as the same number of previously unidentified events. Kriging methods provided spatially explicit estimates of avalanche return periods. Estimated return periods for the entire avalanche path averaged 3.2 years. Within this path, return intervals ranged from ~2.3 yrs in the lower track, to ~9-11 yrs and ~12 to >25 yrs in the runout zone, where the railroad and highway are located. For avalanche professionals, engineers, and transportation managers this technique proves a powerful tool in landscape risk assessment and decision making.

KEYWORDS: avalanche history, tree-rings, kriging, return periods.

1. INTRODUCTION

In this paper we describe new combinations of techniques that enable avalanche professionals to quantify the frequency of past avalanches and to map the spatial extent of those past avalanches. This knowledge will enhance the evaluation of risks and hazards to people and infrastructure in heavily used transportation corridors through mountains.

Snow avalanches onto railroads and highways can be costly in terms of damage to infrastructure and in obstructing delivery of goods and materials. People have historically built roads and other structures in proximity to avalanche paths without any clear knowledge of the frequency and extent of avalanches. In John F. Stevens Canyon, at the southwestern corner of Glacier National Park (GNP), Montana (Figure 1), avalanches have damaged infrastructure and disrupted railroad and highway traffic since at least 1910 (Reardon et al, 2004). Among the most severe accidents are the deaths of three railroad workers in 1929, the burial of two highway workers in 1950, extensive damage to several snowsheds and a locomotive in 1956 and 1957, the destruction of a highway bridge in 1979, and the derailment of a freight train in 2004. Annually the trains carry a total of 61 million tons of freight through the canyon, mostly comprised of grain and shipping containers (Reardon et al., 2004). However, some trains haul hazardous materials and, on a daily basis, water treatment chemicals that are bound for Seattle, Washington. The city of Seattle relies on daily shipments because of minimal storage capacity at treatment plants. Additionally, Amtrak passenger trains traverse the canyon twice daily (Reardon et al., 2004). Thus there is great interest in mitigation of hazard due to 1) the direct and indirect threats to human safety, 2) economic impacts associated with track closure, and 3) on-time delivery of materials for zero inventory systems. The region has experienced rapid population growth of 23% per decade and increasingly relies on expanding tourism. As a

* *Corresponding author address:* Gregory T. Pederson, 106 AJM Johnson Hall, Big Sky Institute, Montana State University, Bozeman, MT 59717; tel: 406-994-7023; fax: 406-994-5122; email: gpederson@montana.edu

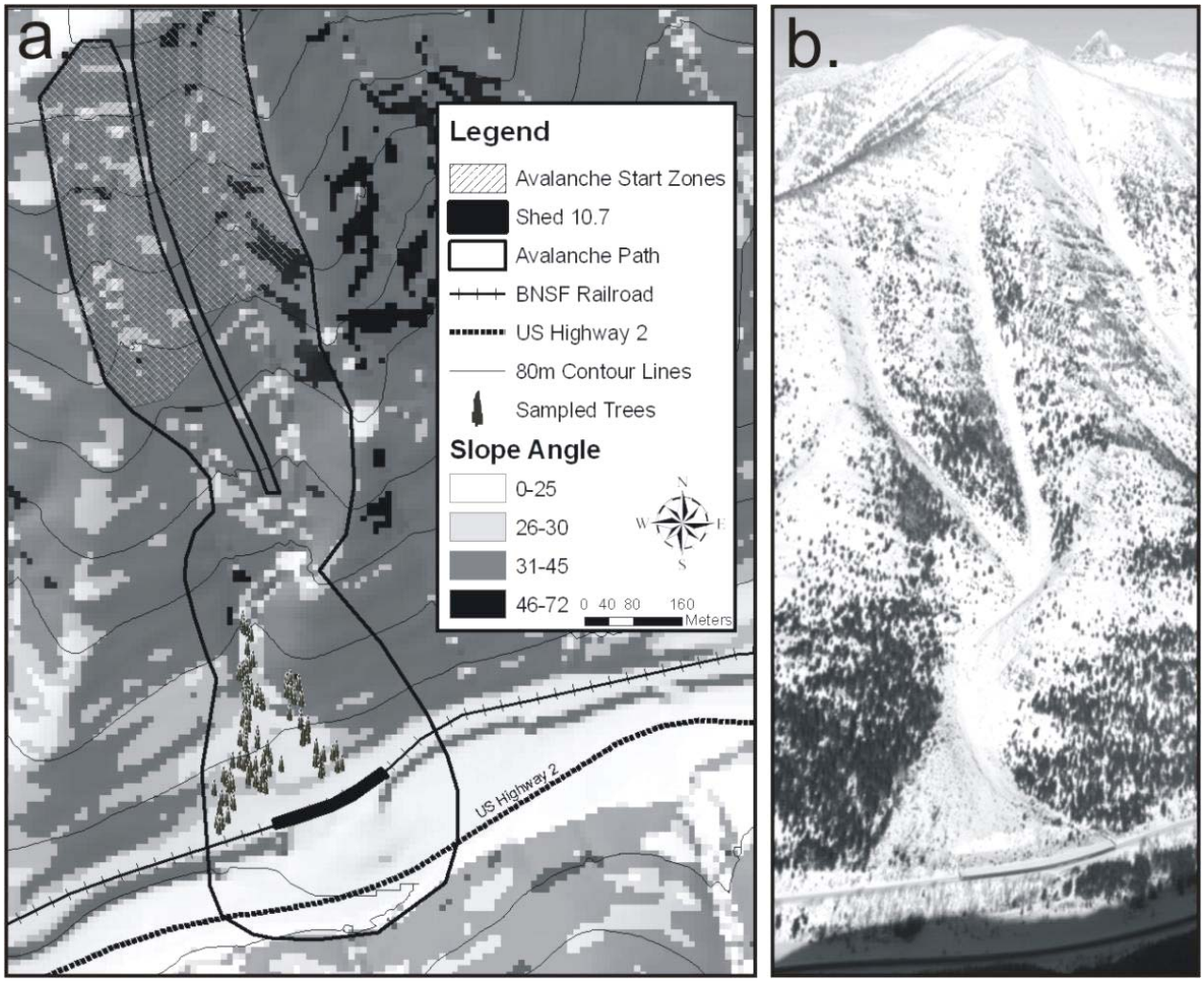

Figure 1: Map of a) slope angles and tree sampling area above Shed 10.7 and U.S. Highway 2, and b) oblique photo of shed 10.7 avalanche path. Photo by Darwon Stoneman, January 2004.

result, highway traffic through the canyon is expected to continue growing and will add to the impacts that snow avalanches have on this transportation corridor.

Until 2005, hazard mitigation in Stevens Canyon was limited to the nine existing snowsheds protecting the railroad track. The lack of direct avalanche control constitutes a unique opportunity to compile a rare long-term record of natural avalanche activity. A heightened recognition of the safety and economic liabilities associated with avalanche hazard in the canyon was prompted by the 2004 closure of the highway and railroad due to a large avalanche. A risk analysis (Hamre and Overcast 2004) was commissioned, mitigation measures were proposed, and an Environmental Impact Assessment was begun as part of efforts to develop an integrated management plan for avalanche hazard. A key component of evaluating risks associated with avalanches is to know their frequency and magnitude. Thus, there is an urgent need for developing a detailed chronology of natural avalanche frequency so that overall risk can be known and appropriate actions taken.

However, the historical record is relatively incomplete, even for avalanches that disrupted traffic on the highway or railroad (Reardon et al., in review). Avalanches were not consistently reported by number, size, or location. Although there is no question that many avalanches went unreported, the extent of the underreporting is not known and, therefore, the extent of risk is difficult to estimate. Hamre and Overcast (2004) attempted to rectify this information gap by making a general estimate of avalanche frequency for Stevens Canyon. They derived the return period of avalanches from numerous paths using the

historic record and tree-ring analysis. However, their sample size per path was limited due to the scale of project, precluding high-resolution spatial analyses of past avalanches in any of the paths. Such spatially-explicit knowledge is needed to develop an understanding of overall avalanche hazard.

We conducted a pilot study on one avalanche path to determine if a high-resolution record of natural avalanche frequency could be developed for the past century by using tree-ring analysis. We also evaluated whether we could reconstruct the spatial extent of those avalanches as a proxy measure of the size of the avalanches.

2. METHODS

The study site – the Shed 10.7 avalanche path (Figure 1a,b) – was selected because recent large-magnitude avalanches (2002 and 2003 winters) killed or injured dozens of trees, yet left the trunks and boles *in situ* or within several meters of their original position. The numerous dead trees allowed destructive sampling (tree cross-sections and wedge samples of impact scars), which provides the most reliable identification and dating of avalanche-induced tree responses (Carrara, 1979). Also, the fact that the trees remained *in situ* enabled precise recording of each sample location using a hand-held GPS unit, which in turn allowed high-resolution mapping of sample depth, minimum avalanche extent in a given winter, and estimated avalanche frequencies within the runout zone.

The Shed 10.7 avalanche path (Figure 1a,b) lies on the steep southern slopes of Running Rabbit Mountain (2347 m a.s.l.). The main start zone lies between 2070 and 2190 m a.s.l. (Hamre and Overcast, 2004). The track is steep and confined, with an s-curve at the bottom. Below the curve, the path transitions abruptly into a broad, fan-shaped runout zone cut longitudinally by a shallow, tree-less gully. The snowshed and railroad cross the bottom of this fan at 1270 m a.s.l. The slope drops steeply from the railroad to U. S. Highway 2, which runs through the floodplain of Bear Creek at 1235 m a.s.l. Total vertical fall from the main start zone to Bear Creek is 955 m, with an alpha angle of 27 degrees. A tributary start zone and track run just west of the main path. The tributary track falls 450 vertical m to a confluence with the main track just above the bottom of the s-curve.

Many trees within the runout zone exhibit signs of damage from multiple avalanche events. The trimline along the western edge is abrupt, while along the eastern edge, the transition from avalanche path to forest is more gradual. The dominant tree species is Douglas-fir (*Pseudotsuga menziesii*), with quaking aspen (*Populus tremuloides*), lodgepole pine (*Pinus contorta*) and western larch (*Larix occidentalis*) also present. Above the railroad, the Shed 10.7 path lies within GNP (est. 1910). Park management policies limit human activities within the path and thus the potential for human-caused tree damage that could be mistakenly attributed to avalanches. Wildfires that could affect a tree-ring record from the path include a large, stand-replacing wildfire in 1910 and several smaller wildfires in the 1920s (Barrett, 1986). Scars and charcoal were evident on some dead trees found in the forest west of the avalanche path, and the oldest tree sampled for this study dated to 1910.

2.1 Historic record

Reardon et al. (2004) compiled a 95-year chronology of historic avalanches in Stevens Canyon that includes 13 avalanche events known to have occurred in the Shed 10.7 path. Sources consisted of personal interviews and historic documents and photographs from GNP, the Great Northern Railway, Montana Department of Transportation, and local newspapers. The historic record also includes 15 other avalanche events that we classified as possibly occurring in the Shed 10.7 path. Possible avalanche events were those for which the record indicated an avalanche occurred in the immediate vicinity of Shed 10.7 but the evidence was insufficient to confirm Shed 10.7 as the precise location, or those for which the record listed multiple avalanches within the canyon on a given date but did not give locations.

2.2 Sample collection

We sampled 109 trees located in the lower track and upper runout zone of the Shed 10.7 avalanche path (Figure 1a). Three types of samples were collected: (1) cross-sections from dead trees, (2) cross-sections from the dead leaders of avalanche-damaged but still living trees, and (3) cores from living trees. GPS coordinates with sub-1m accuracy were recorded for each sampled tree using a Trimble GeoExplorer XT®.

Notes described the amount of impact scarring, branch flagging, tilting and other salient characteristics of each sampled tree.

Sample types (1) and (3) were collected as close to the root buttress as possible. This practice provides accurate estimates of establishment dates and captures reaction wood (i.e. colored wood tissues produced when a tree responds to impact or tilting with asymmetrical growth). For all three types, we sampled visible scars resulting from the impacts of avalanche debris. Samples were collected at random from the majority of available *in-situ* trees of all species within and along the margins of the Shed 10.7 avalanche path. No samples were collected below the snowshed or railroad, where railroad and highway maintenance and other human activities have damaged trees, resulting in growth responses that could be mistakenly ascribed to avalanches.

Cross-sections were collected from 67 dead, *in-situ* trees, and comprise the majority (62%) of our samples. These samples came from trees with intact root wads and trunks that were oriented roughly parallel to the flow path of the slope, indicating they were likely killed in an avalanche. A smaller number of cross-sections (n=24; 22%) were collected from the dead leaders of avalanche-topped trees where cambial growth was still active. This technique maximized data collection from frequently impacted living trees in the lower track of the avalanche path while avoiding damage due to sampling. Lastly, 18 live trees (16%) showing obvious avalanche damage (e.g. tilting, impact scarring, and branch flagging) were sampled using an increment borer. Four cores were removed from each tree, two perpendicular and two parallel to the fall-line of the slope. This procedure helped in the detection of growth anomalies and reaction wood in core samples.

2.3 Sample processing and analysis

All samples were processed using standard dendrochronology procedures (Stokes and Smiley, 1968). Missing and/or false rings were accounted for, and accurate dating was statistically verified using the COFECHA program (Grissino-Mayer et al. 1997). For samples heavily impacted by multiple avalanches, avalanche "marker years" recorded in neighboring samples (e.g. 1993 and 2002 avalanche events) ensured accurate calendar dating.

We then rated each avalanche-induced growth response/injury from 1-5 based on the visual quality of scars or reaction wood within each sample. This tree-growth response rating system allowed the data to be filtered by sample quality during analysis; it is outlined below:

1. Clear impact scar associated with obvious reaction wood or growth suppression.
2. Clear scar, but no reaction wood or suppression of growth, OR, obvious reaction wood/suppression of growth that occurs abruptly after complacent or "normal" growth and that lasts for approximately three years.
3. Well-defined reaction wood/suppression of growth, but only prevalent in 1 or 2 successive growth years.
4. Reaction wood or growth suppression present but not well defined, OR, reaction wood present but formed when tree was young and more susceptible to damage from various environmental and biological conditions.
5. Same as 4 except reaction wood is very poorly defined, and slow onset may indicate other processes such as soil or snow creep may be primary causes.

Once the quality of recorded events was assessed, event-response histograms were produced following Dube et al. (2004). Two histograms were calculated by using (1) the raw number and (2) the percentage of trees (calculated from total number of living trees in year t) recording an event through growth responses. Thus, the index I is calculated for each year t as follows:

$$I_t = \left(\left(\sum_{i=1}^{n} Rt \right) \div \left(\sum_{i=t}^{n} At \right) \right) \times 100 \qquad (1)$$

where R represents a tree's response to an event in year t, and A is equivalent to the number of trees alive in that year t. To classify an event as an avalanche year based solely on growth responses, we required that ten or more trees exhibit a response and that the index I be ≥10% of the samples alive at year t. The first threshold reduced the potential for overestimation - noted by Dube et al. (2004) - that can occur with decreased sample depth early in the record. The second minimized the chance that growth anomalies caused by non-avalanche events such as rockfall would mistakenly be ascribed to avalanches. A year was

automatically classified as an avalanche year if the historic record listed a known avalanche in Shed 10.7 that winter.

2.4 Calculations of natural avalanche return periods and extent

Avalanche frequency is the average number of times within a time period that debris reaches a given point in an avalanche path (McClung and Schaerer, 1993). Frequency is usually expressed in years as a "return period" (1/frequency). For this study, we calculated return periods for each tree within the path, and then for the entire lower section of the path by combining the individual tree return period estimates with the spatial data in ArcMap 9.2 (ESRI 2005). Individual tree return periods were calculated from the growth response frequency *f* for each tree *T* as follows:

$$f_T = \left(\sum_{i=T}^{n} Gr\right) \div \left(\sum_{i=T}^{n} A\right) \qquad (2)$$

where *Gr* represents the number of growth responses, and *A* the total number of years tree *T* was alive. Return Periods were next mapped using various kriging methods to ensure robust spatial estimates. Exploratory visualizations of avalanche return periods were performed using inverse distance weighting. This helped ensure interpolated avalanche frequency patterns produced using the kriging method did not result solely from parameterization of the model. With properly selected parameters, the kriging method uses the spatial autocorrelation between sampled trees to produce spatially accurate estimates of avalanche return periods. Here, the best-fit model of avalanche return periods was produced using ordinary kriging methods and a spherical semivariogram. The lag (or bin) size was set to 27.75 m with 12 lags to optimize the fitting of the semivariogram. Due to the strong directional influence (i.e. points are closely related to those upslope of their location), anisotropy was set using an angle direction of 0°, an angle tolerance of 45° and a bandwidth of 6. For estimating the avalanche frequency of a point on the landscape, an ellipse-shaped search neighborhood used at least five, and up to 25 weighted points, within each of its eight sectors.

The database of sample locations, and thus growth responses by year, was also used to investigate questionable avalanche years, and to estimate minimum avalanche extent for each year classified as an avalanche event. Minimum avalanche extent estimates were developed by mapping all trees showing and not showing growth responses in the specific avalanche year.

3. RESULTS

3.1 Comparison of tree-ring and historic avalanche chronologies

Overall, we were successful in finding enough trees for the method to provide a detailed and accurate avalanche chronology from impact scars and reaction wood. However, the record's length is ultimately limited due to problems related to sample depth over the early portions of the chronology. At all avalanche sites material is continually lost due to successive avalanche events, and the larger and more frequent the avalanches at a particular site became, the shorter the tree-ring based historical record ultimately became. In Shed 10.7 the oldest of the 109 samples dated to 1910. In 1936 the sample depth surpassed the n ≥ 10 trees threshold for growth responses to be classified as an avalanche event using the tree-ring record alone. The sample depth increased markedly after 1965 and surpassed 50% (n=55) in 1972.

Combining the tree-ring and historic records yielded a total of 27 avalanche years in the 94-year chronology (1910-2003), more than doubling the number of confirmed avalanches in Shed 10.7 over the historic record alone. From 1910-1936, the tree-ring record showed growth-responses in only three years, with one of those coinciding with a known historic avalanche event (n=9) and none coinciding with possible but unconfirmed avalanche events (n=2). After 1936, the tree-ring record included growth responses that are ≥ 10% of samples in all known historic avalanche years (n = 4) and many years that were either possible but unconfirmed (n = 9), or absent from the historic record (n = 5). In all but two of these cases – known avalanche years 1947 and 1957 – 10 or more trees recorded growth responses. We removed six possible avalanche years from the avalanche chronology when < 10 trees and < 10% of the total samples alive that year recorded responses.

The quality assurance steps (e.g. requiring ≥ 10% or ≥ 10 trees record any particular avalanche event) eliminated many potential

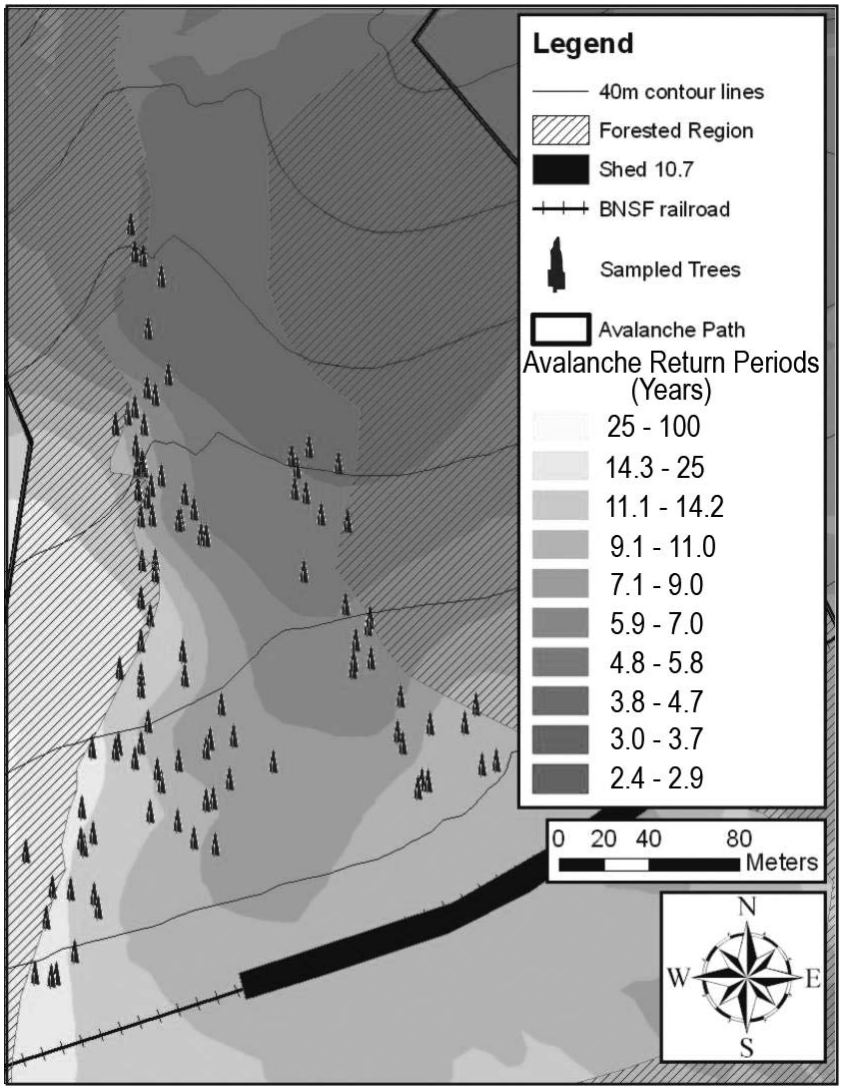

Figure 2. Interpolated return periods for the sampled area of the Shed 10.7 runout zone.

avalanche years, indicating that our method is conservative. Had we lowered the standards, more years would have been classified as avalanche years resulting in an even greater amount of underreporting by the historic record. This, however, would have also resulted in a much higher number of incorrectly identified avalanche years and biased estimates of avalanche frequency.

3.2 Spatially explicit avalanche return period estimates

With the spatially accurate locations of tree samples provided by the GPS, we were able to produce maps showing an estimate of minimum avalanche extent for each avalanche year. The greatest power of this method, however, was the ability to create spatially explicit maps of avalanche return periods (1/frequency). Figure 2 clearly demonstrates the much higher frequency of avalanche events at higher elevations within the path, as well as the frequency with which the tracks are impacted, or nearly impacted by avalanche debris.

Non-spatial estimates of avalanche return periods generated from this dataset indicate that on average Shed 10.7 slides every 3.2 yeas. However, this estimate is misleading for engineering and management purposes. The more accurate spatial estimate of avalanche return periods generated by kriging the data produces a more informative map of avalanche frequencies within the avalanche path (Figure 2). Within the

avalanche path, return periods increased rapidly with distance down slope, particularly at the bottom of the debris fan immediately above the snowshed. The map of avalanche return periods within the sampled area showed calculated return periods (1/f) ranging from 2.3 years in the lower track to 25 years for the unprotected section of the railroad in the runout zone. The horizontal distance between these points is less than 300m, with an elevation change of only 125m. In the upper 40 vertical meters of the runout zone, return periods increased by only a year, from 4.8 to 5.9 years, yet nearly doubled in the remaining 50 vertical meters above the snowshed, to 11.1 years.

4. DISCUSSION

These methods are useful for avalanche professionals, engineers, and transportation managers because they provide realistic, if not conservative, estimates of avalanche impact risk distributed across a landscape. An evaluation of risk in Stevens Canyon based on historic documents alone not only lacks useful information related to spatial expression of avalanche events, but also underestimates avalanche return periods by a factor of 2. By integrating information gleaned from historic documents with accurately mapped avalanche extents derived from tree-ring data, a more valuable estimate of natural avalanche frequency can be produced. This in turn enhances the ability to make decisions about appropriate levels of risk, and ultimately whether to tolerate or mitigate a potentially large hazard. In addition to the safety of travelers and railroad workers, there are substantial economic and societal liabilities that demand consideration. Better risk assessments should directly support improved decisions and hazard mitigation across this complex, multi-jurisdictional landscape.

Spatial mapping of avalanche return periods also helps to shape understanding of how frequent avalanches are by size, and how avalanche return period (and risk) varies by position on the slope. From a structural engineering prospective this potentially helps in locating infrastructure in the future, and for evaluating risk to present infrastructure. For example, Figure 2 shows that Shed 10.7 protects the majority of the railroad track from the most often impacted (approximately every 11-15 years) portion of the avalanche runout zone. The map also suggests to transportation managers that the remaining exposed portions of track will be vulnerable to avalanches with return periods between 15 years and 100 years.

5. CONCLUSIONS

Tree-ring based analysis techniques are well established but, when applied intensively along with GIS and GPS technology to a single avalanche path, revealed important information that historic records did not. Although the field collection of this data can be completed relatively rapidly (e.g. the data for this study was collected by three of the investigators over four days), there is a substantial expense involved in processing the samples, performing rigorous quality assurance and control, and finally analyzing the data. Nonetheless, this effort allowed for an assessment of avalanche return periods to be quantified across the landscape. For the Shed 10.7 avalanche path there is now a greater understanding of avalanche return periods that may be used in future risk analysis, mitigation planning and decision making, or, perhaps alert current managers of previously unknown problems related to the existing shed.

Thus, we conclude that this is clearly a worthwhile technique to add to the arsenal of tools that avalanche professionals can use to evaluate hazards in mountain environments with high spatial resolution, and to better design programs to manage the risk.

6. ACKNOWLEDGMENTS

We gratefully acknowledge support from the staff at Glacier National Park and the Big Sky Institute at Montana State University. This work is a contribution of the U.S. Geological Survey Global Change Research Program's Western Mountain Initiative

7. REFERENCES

Barrett, S. W., 1986: Fire history of Glacier National Park: Middle Fork Flathead River drainage: Final report. *National Park Service*, Glacier National Park, West Glacier, MT, 32 pp.

Carrara, P. E., 1979: The determination of snow avalanche frequency through tree-ring analysis and historical records at Ophir, Colorado. *Geological Society of America Bulletin*, Part I, 90: 773-780.

Dube, S., Filion, L., and Hetu, B., 2004: Tree-ring reconstruction of high-magnitude snow avalanches in the northern Gaspe Peninsula, Quebec, Canada. *Arctic, Antarctic and Alpine Research*, 36: 555-564.

Environmental Systems Research Institute (ESRI), *ArcGIS 9.2*, Redlands, CA (1992-2006).

Hamre, D. and Overcast, M., 2004: Avalanche Risk Analysis, John Stevens Canyon, Essex, Montana. Girdwood: *Chugach Adventure Guides*. 74 pp.

Grissino-Mayer, H.D., R.L. Holmes, and H.C. Fritts. 1997. The International Tree-Ring Data Bank Program Library. *Version 2.1, users' manual*, Tucson, AZ, 106 pp.

McClung, D. M. and Schaerer, P. A., 1993: The Avalanche Handbook. Seattle: *Mountaineers*. 271 pp.

Reardon, B. A., Fagre, D. B., and Steiner, R. W., 2004: Natural avalanches and transportation: a case study from Glacier National Park, Montana, U.S.A. In *Proceedings of the International Snow Science Workshop*, Jackson, Wyoming. In Press.

_____, B. A., G. T. Pederson, C. J. Caruso, and D. B. Fagre, In review: Spatial reconstructions and comparisons of historic snow avalanche frequency and extent using tree-rings in Glacier National Park, Montana, USA. *Arctic, Antarctic and Alpine Research*. In review.

Stokes, M. A. and Smiley, T. L., 1968: An introduction to tree-ring dating. Chicago: *University of Chicago*. 73 pp.